JOURNAL OF GEOPHYSICAL RESEARCH, VOL. 103, NO. E10, PAGES 22,831–22,845, SEPTEMBER 25, 1998

The composition of the Jovian atmosphere as determined by the Galileo probe mass spectrometer

H. B. Niemann,[1] S. K. Atreya,[2] G. R. Carignan,[2] T. M. Donahue,[2] J. A. Haberman,[1] D. N. Harpold,[1] R. E. Hartle,[1] D. M. Hunten,[3] W. T. Kasprzak,[1] P. R. Mahaffy,[1] T. C. Owen,[4] and S. H. Way[1]

Abstract. The Galileo probe mass spectrometer determined the composition of the Jovian atmosphere for species with masses between 2 and 150 amu from 0.5 to 21.1 bars. This paper presents the results of analysis of some of the constituents detected: H_2, He, Ne, Ar, Kr, Xe, CH_4, NH_3, H_2O, H_2S, C_2 and C_3 nonmethane hydrocarbons, and possibly PH_3 and Cl. $^4He/H_2$ in the Jovian atmosphere was measured to be 0.157 ± 0.030. $^{13}C/^{12}C$ was found to be 0.0108 ± 0.0005, and D/H and $^3He/^4He$ were measured. Ne was depleted, ≤0.13 times solar, Ar ≤1.7 solar, Kr ≤5 solar, and Xe ≤5 solar. CH_4 has a constant mixing ratio of (2.1 ± 0.4) × 10^{-3} (^{12}C, 2.9 solar), where the mixing ratio is relative to H_2. Upper limits to the H_2O mixing ratio rose from 8 × 10^{-7} at pressures <3.8 bars to (5.6 ± 2.5) × 10^{-5} (^{16}O, 0.033 ± 0.015 solar) at 11.7 bars and, provisionally, about an order of magnitude larger at 18.7 bars. The mixing ratio of H_2S was <10^{-6} at pressures less than 3.8 bars but rose from about 0.7 × 10^{-5} at 8.7 bars to about 7.7 × 10^{-5} (^{32}S, 2.5 solar) above 15 bars. Only very large upper limits to the NH_3 mixing ratio have been set at present. If PH_3 and Cl were present, their mixing ratios also increased with pressure. Species were detected at mass peaks appropriate for C_2 and C_3 hydrocarbons. It is not yet clear which of these were atmospheric constituents and which were instrumentally generated. These measurements imply (1) fractionation of ^4He, (2) a local, altitude-dependent depletion of condensables, probably because the probe entered the descending arm of a circulation cell, (3) that icy planetesimals made significant contributions to the volatile inventory, and (4) a moderate decrease in D/H but no detectable change in (D + ^3He)/H in this part of the galaxy during the past 4.6 Gyr.

1. Introduction

The Galileo probe mass spectrometer (GPMS) obtained useful data concerning the composition of the Jovian atmosphere along the probe trajectory between pressure levels of 0.51 and 21.1 bars. Among species detected were H_2 and HD, ^3He and ^4He; the isotopes of the noble gases Ne, Ar, Kr, and Xe; the volatiles CH_4, NH_3, H_2O, H_2S; a chlorine compound which may have been HCl, and a large number of C_2 and C_3 nonmethane hydrocarbons (NMHCs). Mixing ratios, or data capable of being translated into mixing ratios, have been obtained from the mass spectra acquired by direct sampling of the atmosphere and information provided by two enrichment cells for numerous species. Striking aspects of the abundance profiles were (1) the very low mixing ratios of condensable volatiles such as H_2S and H_2O at pressures <8 bars and their gradual increase at higher pressures along the probe trajectory, (2) the suggestion that the mixing ratio of H_2O may imply subsolar ^{16}O at the entry site even near 20 bars, (3) mixing ratios of S and C of 2.5 or 3 times solar at high pressure, and (4) depletion of helium and neon relative to their solar abundances. The elemental solar abundances referred to in this paper are taken from *Anders and Grevesse* [1989].

A precise measurement of the $^4He/H_2$ ratio was obtained that shows atmospheric helium is slightly depleted in the Jovian atmosphere relative to protosolar helium. $^{13}C/^{12}C$ was among the isotopic ratios measured. The important light element ratios D/H and $^3He/^4He$ have previously been reported by *Mahaffy et al.* [1998] to be (2.6 ± 0.7) × 10^{-5} and (1.66 ± 0.05) × 10^{-4}, respectively. All the quantities given here supersede those in our preliminary report [*Niemann et al.*, 1996].

2. Instrument

The GPMS has been described in detail [*Niemann et al.*, 1992]. A quadrupole mass filter scanning in integral mass steps from 2 to 150 atomic mass units (amu) provided mass analysis. A one half-second integration time was allotted to each mass step. A secondary electron multiplier detected the ions transmitted by the mass filter. The ion arrival rate at the detector during each half-second constituted the primary measurement. Pulse counting rates per step varied from 0 to about 1.2 × 10^7 when the atmosphere was being sampled directly and to more than 5 × 10^7 during enrichment cell exercises. Because of the nonvanishing recovery time of the pulse counting system after a pulse was received, an appreciable correction needed to be applied to the raw count rates at their higher levels. This corrected count rate was derived from the expression

$$[o] = [m] \exp(-[m]/[m]_0)$$

[1]Goddard Space Flight Center, Greenbelt, Maryland.
[2]Department of Atmospheric, Oceanic and Space Sciences, University of Michigan, Ann Arbor.
[3]Lunar and Planetary Laboratory, University of Arizona, Tucson.
[4]Institute for Astronomy, University of Hawaii, Honolulu.

Paper number 98JE01050.
0148-0227/98/98JE-01050$09.00

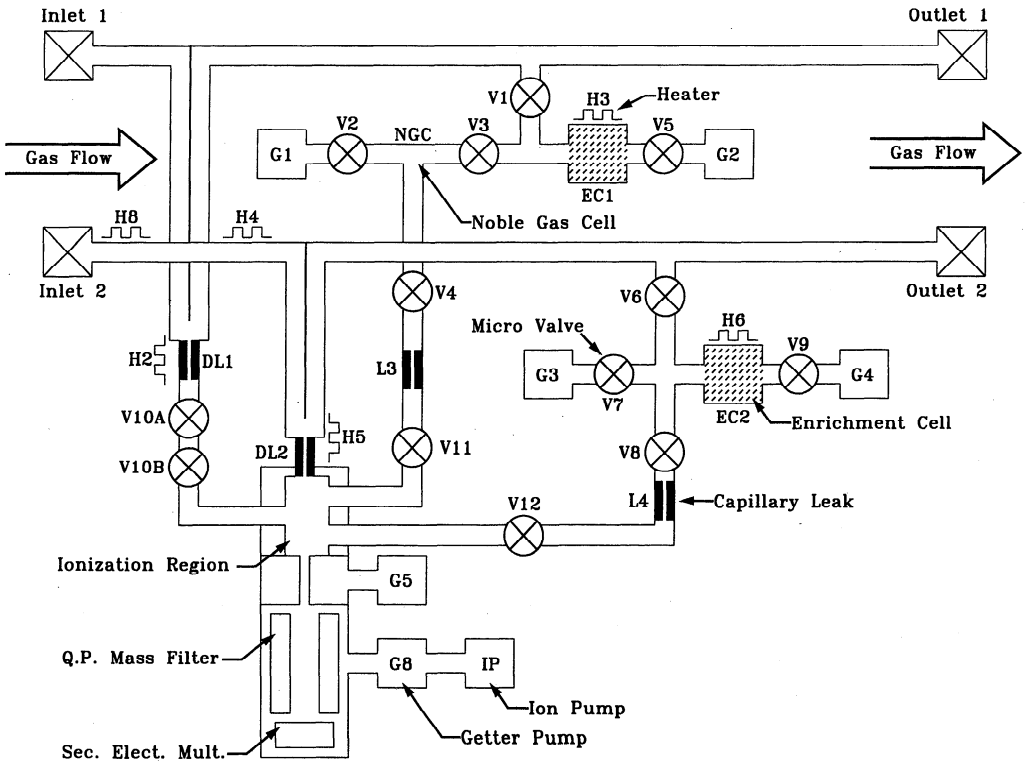

Figure 1. Schematic diagram of the gas inlet system to the mass spectrometer.

where $[o]$ is the measured number of counts per step at m amu, $[m]$ is the corrected count rate, and $[m]_0$ was empirically determined as 2.933×10^7 c/step (counts per step). This correction is no longer valid when the rates are in excess of about 1×10^7 c/step. Since the determination of mixing ratios required measurement of the ratio of counting rates for a selected species and the rates for H_2 or ^4He, it was necessary to use a secondary standard at high pressure levels where 4 and 2 amu corrected count rates exceeded 10^7 c/step. Selection of an appropriate secondary standard is discussed in section 6 of this paper.

The instrument was under the control of a sequencer with read-only memory (ROM). The ROM address was incremented at half-second intervals to determine six instrument variables, such as mass number, ionization energy, or inlet system configuration. To verify the mass resolution, a sequence of high-resolution mass scans was implemented at the 17 bar level near the end of the nominal mission sequence. During this sequence, and also during an earlier background measurement, the mass was stepped in intervals of 1/8 amu.

A schematic diagram of the gas handling system and the mass spectrometer part of the instrument is shown in Figure 1. A miniature dual-filament ion source provided a magnetically collimated electron beam to ionize the gas by electron impact. The second filament provided redundancy but was not needed. Three values of electron beam energy were available. Usually the energy was set at 75 eV, but on occasions it was decreased to 25 or 15 eV for diagnostic purposes. The ion source chamber was very compact and separately pumped by a nonevaporable-getter pump. A high-capacity baffled getter pump in cascade with a sputter ion pump also pumped the mass filter and detector chamber. The gas flow into the pumps was conductance limited to assure constant pumping speed. This configuration was necessary to provide for the removal of the most abundant species, namely, hydrogen, by the getter pump before the gases arrived at the sputter ion pump. Helium, which is not pumped by the getter, was then buried in the pump cathodes of the sputter ion pump. The production of hydrocarbons on sputter ion pump surfaces that might be regurgitated by the pump was inhibited by this arrangement.

To prepare the instrument for flight after calibration and to erase all memory in this instrument of the calibration gases, all getter pumps, the sputter ion pump, and the enrichment cells were replaced with new units. The enrichment cells were activated by purging with ultrapure helium for several hours at 400°C. The instrument was baked for several days at 280°C on an oil free ultrahigh vacuum system, and the getters were activated at 900°C before the instrument was pinched off from the vacuum system.

Small amounts of background gases in the instrument were ^{40}Ar, CH_4, H_2O, CO, and CO_2. Except for H_2O, all background count rates were below 100 c/step. Prior to launch, a full descent sequence was executed, allowing the enrichment cell heaters to operate at their intended full power levels. No background gases other than the nominal gases cited above were observed, confirming that the instrument was clean. Subsequent instrument turn-ons after launch and during cruise to Jupiter showed a gradual decrease in the remaining low-level background gases.

The instrument was enclosed in a titanium container pressurized with nitrogen gas at 1.2 bars. The weight of the instrument plus the titanium shell was 13.2 kg. Power consumption averaged 25 W, of which 11 W were dissipated in the electronics and the rest by the sputter ion pumps, the ion source filament, and the heaters.

As Figure 1 illustrates, there were two sample inlets, one

used at low pressures (0.508–3.8 bars, steps 83–1811) and the other used in the pressure regime above 8.6 bars. The probe measurement sequence was initiated later than planned, resulting in opening the first gas sample inlet system at 0.5 bar instead of 0.10 bar and the second at 8.6 bars instead of approximately 7.0 bars. Similarly, the enrichment cells were charged at somewhat higher ambient pressure levels than anticipated. Gas entered the systems near the apex of the probe close to the stagnation point and left inside the probe, where the pressure was about 6 mbar lower. After the inlet and outlet seals were broken, gas flowing into the system was admitted to the ionization chamber through a glass capillary leak array designated direct leak 1 (DL1). The leak was designed to maintain the ion source chamber pressure below 10^{-4} mbar. Surfaces in contact with sampled gases were passivated. As the atmospheric gases were being sampled through DL1, the enrichment chamber EC1 and the noble gas enrichment cell (NGC), which was simply the region contained between valves V2, V3, and V4, were charged. The enrichment cell EC1 was packed with material chosen to adsorb complex hydrocarbons but effective also for the noble gases, especially Kr and Xe. Before being charged, the enrichment cells and the NGC were kept in vacuum and pumped by the getters G1 and G2. During charging of EC1, valves V1 and V5 were open and valves V2, V3, and V4 were closed. Thus the EC1 volume was exposed to the ambient atmosphere, and an amount of gas about 10 times the capacity of getter G2 was passed through EC1 because G2 removed all incoming hydrogen until the flow was finally blocked by accumulation of atmospheric helium. Subsequently, valves V1 and V5 were closed, V2 and V3 opened, and reactive gases remaining in the gas phase mostly removed by getter G1, greatly reducing the partial pressure of the atmospherically dominant hydrogen. Then V3 was closed and V4 opened to allow some of the contents of the NGC to flow through leak L3 and valve V11 into the ion source. At the same time, EC1 was heated to desorb the gases trapped on the cell material. These remained in the volume of the enrichment cell and the region enclosed by V1, V3, and V5 until V3 was opened and the trapped gases were added to the contents of the NGC. The second enrichment cell EC2 was operated in a manner similar to EC1, but the noble gas subsystem sampling was not repeated.

The sequence of events as the probe descended can be followed by using Figure 2 and the mass spectra in Figure 3 in conjunction with Figure 1. Figure 2 shows, on a logarithmic scale, the count rate per step at 14 amu as a function of the step number. DL1 was sealed off from the mass spectrometer by redundant valves V10A and V10B at step 1811 (3.8 bars), by which time the 14 amu count rate per step had increased from 4733 to 1.03×10^5 (Figure 2). With V10A, V10B, and V4 closed, the background counting rate in the mass spectrometer enclosure was determined (B1). Typically, counts in B1 were between 0 and 3 per step. Even at 2 and 16 amu the rates were only about 650 and 4000 c/step. A background spectrum had also been obtained before the sequence began at step 83. It revealed a similarly clean instrument. During this period, high-resolution mass scans centered at 4, 16, 28, and 44 amu were also executed.

At step 2161, V4 was opened, and gas in the NGC was sampled through L3. On the high-pressure side of L3 the gas density was sufficiently low that gas entered the leak in free molecular flow. On the other hand, gas flow through the DL1 underwent a transition from free molecular toward viscous flow, as the atmosphere was being directly sampled. Several

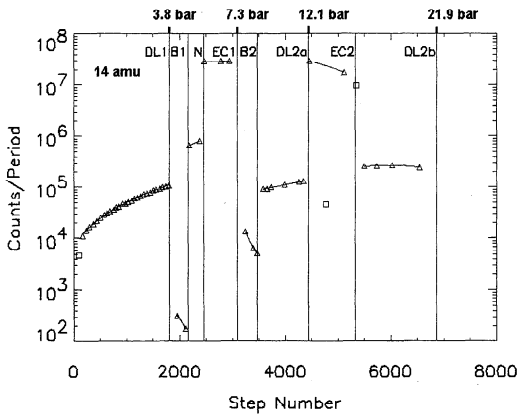

Figure 2. Log of the number of counts per step at 14 amu throughout the probe descent. The continuous lines represent polynomial fits. The square symbols identify measurements that were not included in the fits. Vertical lines separate various modes of instrument operation (DL, direct leak; B, background; N, noble gas; EC, enrichment cell).

spectra in the range 20–40 amu were obtained with the electron energy in the ion source reduced from 75 to 25 eV. At step 3097, V11 was closed, and another background measurement made (B2). During B2, count rates for many species were much higher than in B1 because of the interactions of metal surfaces with gases to which they had been exposed during the EC1 exercise. Ammonia, water, and to a lesser extent, xenon were noticeably affected.

Inlet system 2 was opened at step 3482, when the atmospheric pressure was 8.62 bars. DL2 was designed to minimize gas-surface interactions. The high-pressure flow was sent directly toward the leak, which was located in the ion source cavity, so that the gas entering the chamber had few opportunities to encounter wall surfaces before passing through the electron beam. There was some gas that encountered the walls of the chamber and reentered the ionization region before being removed. Nevertheless, fewer than one in five of the molecules ionized had made contact with the walls. Both inlet systems were heated to temperatures well above those of the ambient atmosphere. Traps were provided for any liquid droplets that may have entered the inlet systems [*Niemann et al.*, 1992]. The measurement period between 8.6 and 12.1 bars will be designated DL2a.

Between steps 4442 (12.1 bars) and 5331 (15.65 bars), V8 was opened, and gas from EC2 was added to the directly sampled gas in the ionization region. This sequence was terminated by closing V12. The electron beam energy was reduced to 25 and 15 eV at times while EC2 was being sampled. By this time, temperatures within the instrument were high (65–70°C), and eventually, especially after step 6000 (18.6 bars), mass-dependent changes in instrument sensitivity began to occur. The last, rather degraded, mass spectrum was obtained between steps 6537 (20.8 bars) and 6657 (21.25 bars). The period after the EC2 exercise will be called DL2b.

Representative samples of mass spectra obtained during probe descent are shown in Figure 3. There were 6637 usable measurements as the probe descended. Because of the need to establish common pressure reference points for each mass spectra, count rates per step for each region were fitted to polynomial functions of the step number at each mass number. Counts per step at m amu will be represented by the symbol

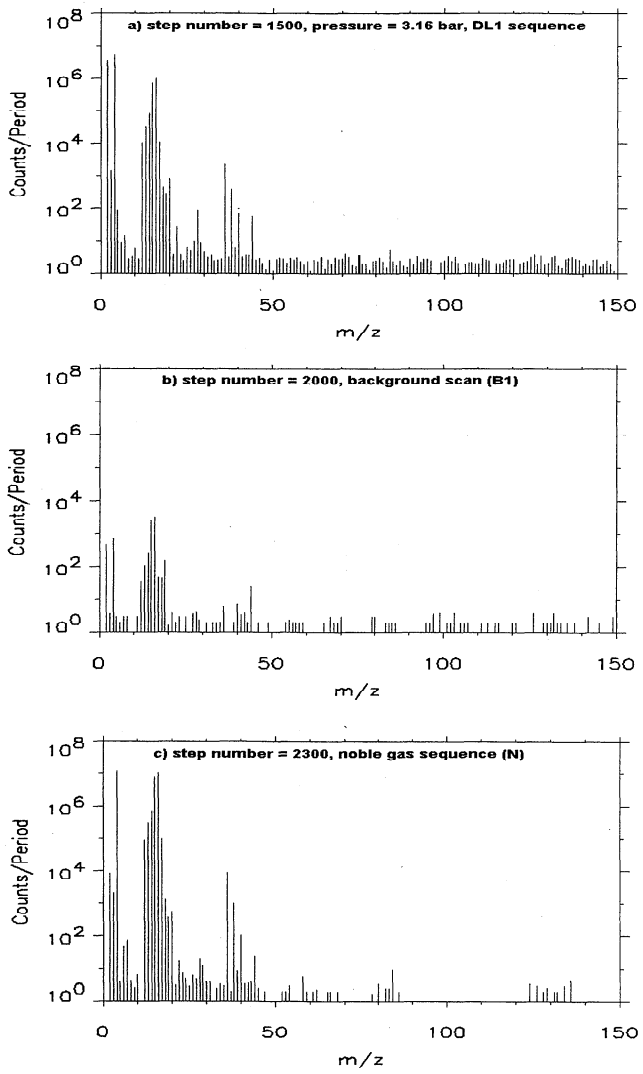

Figure 3. Mass spectra obtained during various stages of the probe descent: (a) DL1 at 3.2 bars, (b) background after DL1, (c) noble gas cell, (d) EC1, (e) background after EC1, (f) DL2a at 9.5 bars, (g) EC2 + DL2, and (h) DL2b at 17.5 bars.

$[m]$. The ratio of $[m]$ to [4], or a suitable proxy for 4 amu, was evaluated and combined with the appropriate calibration factor to generate the mixing ratio of species m relative to H_2. We present our results as mixing ratios (represented by the symbol f), the ratio of number densities to the H_2 number density.

3. Calibration

In 1985, before launch, calibration of the prototype flight unit (PFU) was carried out. The PFU later became the GPMS flight unit (FU). In these, the sensitivity of the FU was determined for a large number of substances that were candidate Jovian atmospheric constituents. The tests were carried out with samples of known concentration added in small known amounts to a predominantly H_2, He or 90% H_2 and 10% He gas mixture. Among species studied were the isotopes of the noble gases, CH_4, PH_3, H_2S, HCN, SiH_4, nonmethane hydrocarbons, NH_3, and H_2O. In one case, discussed in section 4 the inlet pressure and temperature of a mixture of 90% H_2 and 10% He was varied from 0 to 20 bars to simulate the expected entry descent profile.

The laboratory system used to calibrate the GPMS flight unit has now been adapted to calibrate the GPMS engineering unit (EU). Species for which previous calibration data were not available can be studied with this unit, and abundances set to match the Jovian mixing ratios. This calibration system permits gas mixtures to be created and circulated through the inlet lines of the GPMS unit at pressures from several millibars to 22 bars. Pressure gauges of wide dynamic range together with known gas expansion volumes allow mixing ratios down to subparts per billion to be generated in mixtures which represent the Jovian atmosphere with respect to major and significant minor species. Presently, gases from as many as six different tanks can be mixed and introduced into the circulation system.

Calibration for each species of interest is required in order to obtain atmospheric mixing ratios, since the response of the GPMS to each individual species is a function of several factors. These factors include the ion source density for that species, the ionization cross section, the mass spectrometer transmission, and the detector efficiency for each ion. The source density depends on the system pumping characteristics for the particular species of interest and the capillary inlet flow

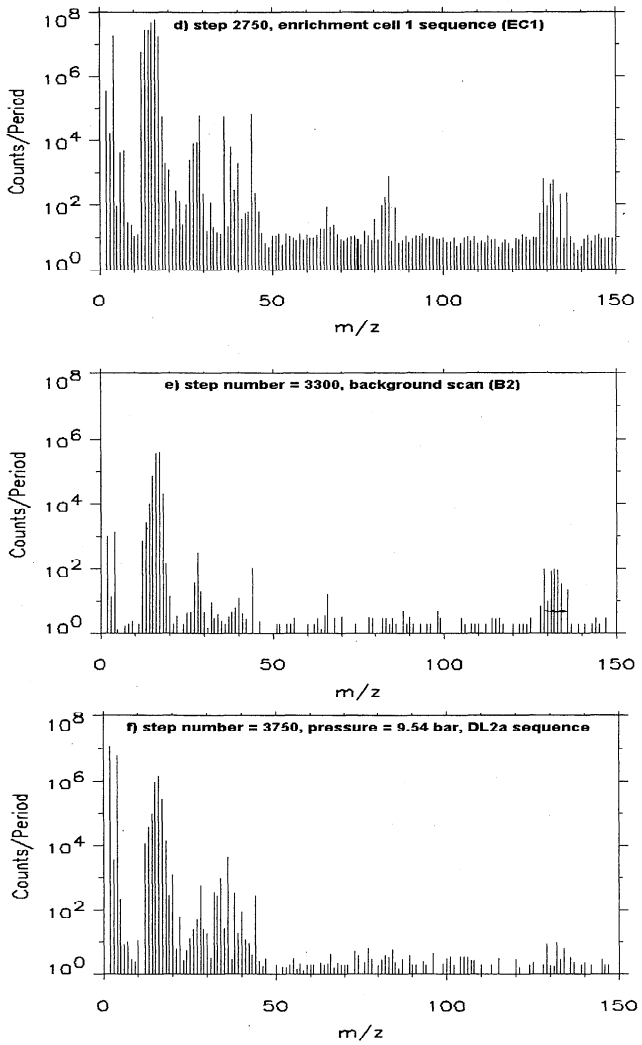

Figure 3. (continued)

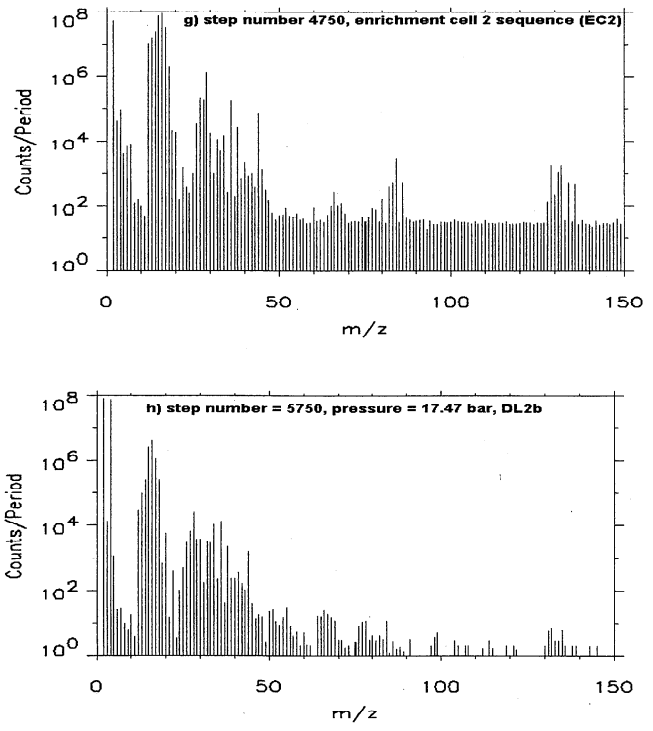

Figure 3. (continued)

characteristics for that inlet pressure. In some cases there are instrument-produced background sources of gas, which must be subtracted. The pumping system used in the calibration of the EU was identical to that used in the FU.

A computer-based data acquisition system allows flexibility in control of the GPMS EU voltages and in data display. Ion and electron focusing lens voltages used in the EU are very close to those used in the FU, with small adjustments made to account for differences in geometry between the ion optical subsystems of the two units. In addition, the GPMS EU is operated with a flight spare radio frequency board to duplicate as closely as possible the behavior of the mass analyzer in the FU. EU elements such as the pumps, enrichment cells, ion source, analyzer, and detector are constructed to the same specifications as those on the FU.

The GPMS sample inlet employed four separate micron-sized capillary leaks. Of these four capillary leaks, two directly sampled the atmospheric gas flowing through the inlet system and two allowed the gas released from the enrichment cells to be introduced into the ion source. The refurbishment of the EU included the installation of enrichment cell leaks with similar gas conductances as the FU. This has allowed EU calibration activities at the very trace levels of krypton and xenon present at Jupiter. However, for all DL2 EU studies reported to date, the conductance of the leak in the EU was a factor of 2 smaller than the FU. This means that ion source densities equivalent to those realized in the 12–22 bar region of the descent (the DL2b region) must be considered tentative until this refurbishment and these studies have been completed.

4. Helium-Hydrogen Ratio

Only H_2 and ^4He contribute effectively to the mass spectra at 2 and 4 amu (Figure 4). Preflight and postflight determination of the sensitivity of the instrument to ions at 2 and 4 amu allowed the ratio of ^4He to H_2 in the Jovian atmosphere to be determined. Thus

$$(^4He/H_2)_c = cc \times ([4]/[2])_J \quad (1)$$

where

$$cc = ([^4He]/[H_2])_c/([4]/[2])_c \quad (2)$$

$([^4He]/[H_2])_c$ is the ratio of helium to hydrogen in the calibration gas and $([4]/[2])_c$ is the ratio of the counting rates produced by this mixture. The results of the calibration exercises were the following sensitivities:

$$\text{DL1:} \quad (cc)_1 = 0.112 \pm 0.020 \quad (3a)$$

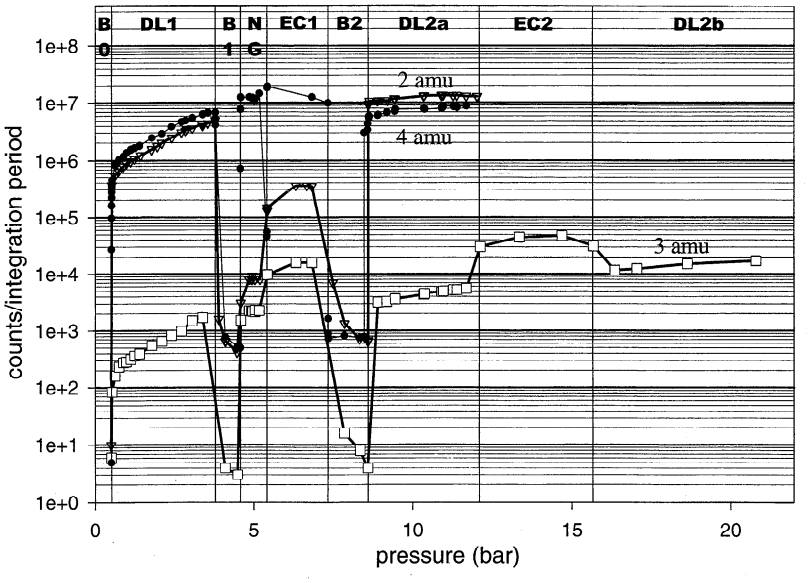

Figure 4. Log of count rates at 2, 3, and 4 amu. The saturation of [2] and [4] at count rates above 2×10^7 per step is apparent.

Table 1. Measured Mixing Ratios or Isotope Ratios

Species or Ratio	Mixing Ratio f or Isotope Ratio	Mole Fraction q	Ratio to Solar
^{4}He	0.157 ± 0.030	0.136 ± 0.026	0.8
^{3}He/^{4}He	$(1.66 \pm 0.05) \times 10^{-4}$		
D/H	$(2.6 \pm 0.7) \times 10^{-5}$		
^{20}Ne	$\leq 3 \times 10^{-5}$	$\leq 2.6 \times 10^{-5}$	≤ 0.13
^{36}Ar	$\leq 10.5 \times 10^{-6}$	$\leq 9.06 \times 10^{-6}$	≤ 1.7
^{84}Kr	$\leq 3.7 \times 10^{-9}$	$\leq 3.2 \times 10^{-9}$	≤ 5
^{132}Xe	$\leq 4.5 \times 10^{-9}$	$\leq 3.8 \times 10^{-10}$	≤ 5
H_2O			
3.6 bars	$\leq 8 \times 10^{-7}$	$\leq 6.9 \times 10^{-7}$	$\leq 4.1 \times 10^{-4}$
12 bars	$\leq (5.6 \pm 2.5) \times 10^{-5}$	$\leq (4.8 \pm 2.1) \times 10^{-5}$	≤ 0.033
19 bars	$\leq (6 \pm 3) \times 10^{-4}$	$\leq (5.2 \pm 2.6) \times 10^{-4}$	≤ 0.35
CH_4	$(2.10 \pm 0.4) \times 10^{-3}$	$(1.81 \pm 0.34) \times 10^{-3}$	2.9
^{13}C/^{12}C	0.0108 ± 0.0005		
NH_3 (>15 bars)	$\leq 2.3 \times 10^{-3}$	$\leq 2 \times 10^{-3}$	≤ 10
H_2S			
3.6 bars	$< 10^{-6}$	$< 8.6 \times 10^{-7}$	< 0.03
8.7 bars	7×10^{-6}	6.1×10^{-6}	0.23
>16 bars	$(7.7 \pm 0.5) \times 10^{-5}$	6.7×10^{-5}	2.5
PH_3 (>16 bar)	$\leq 6 \times 10^{-6}$	$\leq 5.2 \times 10^{-6}$	≤ 8
Cl	detected		

$$\text{DL2:} \quad (cc)_2 = 0.286 \pm 0.040 \tag{3b}$$

The $([4]/[2])_f$ ratios observed at Jupiter were

$$\text{DL1:} \quad [4]/[2] = 1.54 \pm 0.03 \tag{4a}$$

$$\text{DL2:} \quad [4]/[2] = 0.531 \pm 0.010 \tag{4b}$$

The $^4He/H_2$ ratio derived from the GPMS [4]/[2] ratio and a weighted set of DL1 and DL2 calibration constants is

$$\text{DL1 + DL2:} \quad {}^4He/H_2 = 0.157 \pm 0.030 \tag{5}$$

The ratio measured by the Galileo probe helium abundance detector (HAD) (0.157 ± 0.004) reported by *von Zahn et al.* [this issue; *von Zahn and Hunten*, 1996] agrees with this value.

5. Light Isotopes D and ^{3}He

Count rates per step at 2, 3, and 4 amu are shown in Figure 4. From these it is possible to extract the deuterium/hydrogen and ^{3}He/^{4}He ratios in the atmosphere of Jupiter. At 3 amu there were contributions from HD, ^{3}He, and H_3^+. H_3^+ was generated in the ion source by ion molecule reactions involving H_2^+ and by dissociative ionization of methane. Preflight simulation of the entry into the Jovian atmosphere employing a mixture of hydrogen and helium that contained insignificant quantities of ^{3}He and CH_4 and a postflight experiment in which the HD/H_2 ratio was known have been performed. These determined the relative sensitivity of the instrument for HD and H_2 and the amount of H_3^+ present as a function of H_2 partial pressure. Flight data, obtained from background, NGC, and EC exercises, during which hydrogen had been removed from the system by getter pumps, permit a self-consistent determination of the efficiency for production of H_3^+ from CH_4 (very low) and give the helium isotopic ratio [*Mahaffy et al.*, 1998]

$$^3He/^4He = (1.66 \pm 0.05) \times 10^{-4} \tag{6}$$

The GPMS result agrees with the ratio deduced for the protosolar nebula from measurements of (^{3}He/^{4}He) in the planetary component of meteorites $(1.5 \pm 0.3) \times 10^{-4}$ [*Black*, 1972; *Eberhardt*, 1974; *Geiss*, 1993].

With the contributions of H_3^+ and ^{3}He to [3] established, the deuterium/hydrogen ratio can be determined [*Mahaffy et al.*, 1998]:

$$D/H = HD/2H_2 = (2.6 \pm 0.7) \times 10^{-5} \tag{7}$$

This result is in reasonably good agreement with the latest solar wind ratio of $(1.84 \pm 0.5) \times 10^{-5}$ [*Geiss and Gloeckler*, 1998] and the Infrared Space Observatory ratio of $(1.8 \pm 1.1, -0.5) \times 10^{-5}$ [*Encrenaz et al.*, 1996].

6. Noble Gases Ne, Ar, Kr, and Xe

The GPMS obtained data from which the mixing ratios, or upper limits to the mixing ratios, of many volatiles other than hydrogen and helium isotopes could be determined. We present our results as mixing ratios, namely, the ratio of the number density n_i of a given species i to the number density of H_2. We call that ratio $f(m_i)$ for any species m_i. In Table 1 we list both $f(m_i)$ and the mole fraction $q_i(m_i)$, where

$$q_i(m_i) = n_i/(n_{H_2} + n_{He} + \Sigma n_i) \tag{8a}$$

$$q_i \cong n_i/(n_{H_2} + n_{He}) \tag{8b}$$

$$f(m_i) = n_i/n_{H_2} \tag{8c}$$

In DL1 and DL2a the measurement of the mixing ratios began with a determination of the ratio of the counts per step at m_i amu $[m_i]$ to the interpolated counts at 4 amu [4] as previously discussed. This ratio was then multiplied by the laboratory-derived relative sensitivity of the instrument at m_i and [4] for a known mixing ratio $f(m_i)$ relative to H_2, as discussed in section 3. At pressures above 12.1 bars and throughout DL2b (pressure > 15.65 bars), [4] and [2] became so large that the count rate correction became unreliable. Because the mixing ratio of CH_4 was found to be constant with altitude, appropriate candidate secondary standards to substitute for [4] were the CH_4-derived portions of [16], [15], [14], [13], and [12]. Of these, [14], corrected for the contribution from NH_3 and designated [14]′, was selected because the counting rate at 14 amu was large enough, compared to [12], for example, to produce

good statistics and the correction, amounting to 0.0111 [17] as determined by EU exercises, was not large. The relationships between [14]′ and [4] as well as [14]′ and [2] were determined in DL1 and DL2a. Thus

$$\text{DL1:}\quad [4] = 68[14]'$$

$$[2] = [4]/1.55 = 43.9[14]' \tag{9a}$$

$$\text{DL2:}\quad [4] = 69[14]'$$

$$[2] = 1.77[4] = 123[14]' \tag{9b}$$

where

$$[14]' = [14] - 0.0111[17] \tag{9c}$$

Count ratios to [14]′ at 20, 21, 22, 36, and 38 amu did not remain constant with altitude. We continue to study the reasons for this behavior. Under the circumstances, we quote only upper limits for mixing ratios: $^{20}Ne \leq 3 \times 10^{-5}$ (0.13 solar), $^{36}Ar \leq 10.5 \times 10^{-6}$ (1.7 solar). In the case of krypton and xenon, sizeable signals in appropriate mass channels were observed in the NGC, EC1, DL2, and DL2 + EC2 measurements. The ratios to [14]′ (or [4]) were so large that we reported large upper limits for the mixing ratios of these species in our previous paper [*Niemann, et al.*, 1996]. Xenon and krypton are weakly adsorbed on metallic surfaces and the packing of the enrichment cells. This resulted in a slowly decaying background of xenon that was being outgassed from the surfaces during DL2a and DL2b after EC1 and EC2. To a lesser degree, this was also the case for krypton. To derive the Jovian krypton and xenon mixing ratios, it is thus necessary to calibrate the enrichment cells. In laboratory studies with the EU a known quantity of krypton and xenon was added to a mixture of gases of approximate Jovian relative abundances. The enrichment cells were activated, and the response at xenon and krypton mass numbers determined. Preliminary results of these studies give upper limits to the krypton and xenon mixing ratios at Jupiter of 5 times solar abundances, much lower than our previously quoted limits. There is an excellent prospect that these upper limits can ultimately be transformed into measured mixing ratios. The isotopic ratios measured in DL2b are indistinguishable from terrestrial or solar ratios in the case of krypton and xenon, although the xenon ratios are marginally more like terrestrial than solar ratios. For example, the relative abundances of the species at 129 and 132 amu are compared in Table 2.

7. Nonnoble Gas Volatiles

The GPMS obtained data that could be used to determine the value of mixing ratios or set limits on them for CH_4, NH_3, H_2O, H_2S, PH_3, SiH_4, and a compound of Cl along the entry trajectory. The ratios of count rates per data frame at 16, 17, and 18 amu to [14] are shown in Figure 5.

Table 2. Xenon Isotope Ratios

Isotope	GPMS	Terrestrial [*Pepin*, 1991]	Solar [*Anders and Grevesse*, 1989]
129 amu	0.259 ± 0.013	0.254	0.273
132 amu	0.277 ± 0.014	0.274	0.265

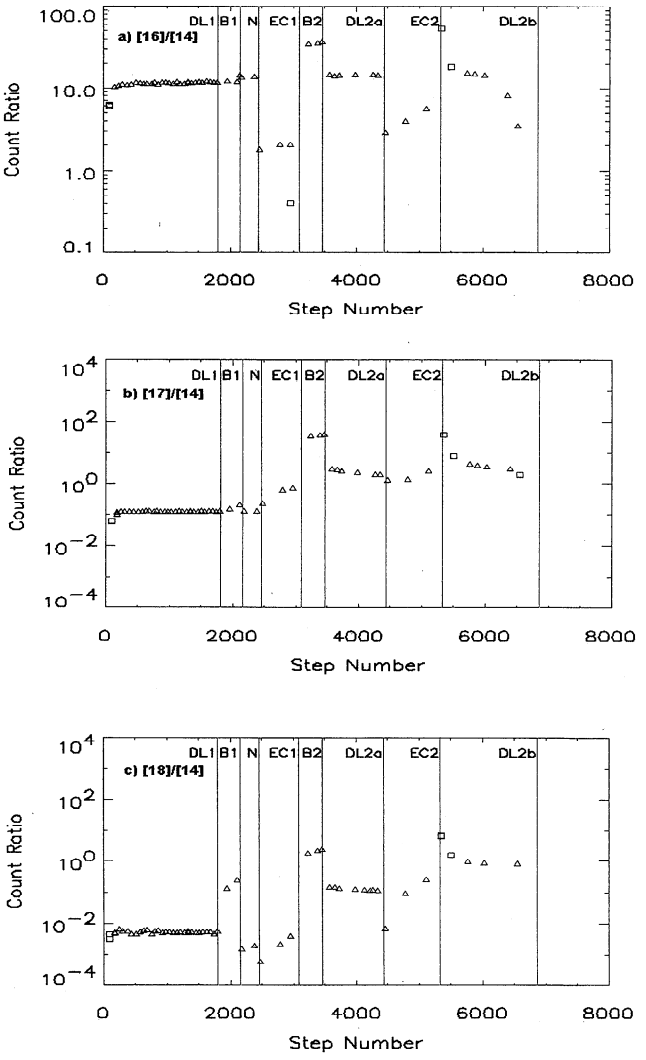

Figure 5. Ratio of counts per step at (a) 16, (b) 17, and (c) 18 amu to counts per step at 14 amu.

7.1. Methane

In the case of methane in DL1 the ratio of [16] to [14] was constant at 11.45 ± 0.34 (Figure 5a). No interfering species, such as H_2O or CH_4, were reaching the detector in appreciable amounts (Figures 5b and 5c). The calibration factor that converts this ratio to a mixing ratio as determined in EU studies was (1.84 ± 0.37) × 10^{-4}. Hence the mixing ratio of methane in the region where the probe entered was

$$f(CH_4) = (2.1 \pm 0.4) \times 10^{-3} \tag{10}$$

In the DL2 region, at pressures greater than 8.62 bars analysis is somewhat complicated by the presence of interfering species at 17 and 18 amu. In DL2b the mixing ratio of CH_4 can, in principle, be determined if a secondary standard, not derived from methane, is used to replace [4]. Unfortunately, none seems to be available. Thus in the region of Jupiter's atmosphere where the Galileo probe entered, ^{12}C was measured to be 2.9 times as abundant as in the Sun [*Anders and Grevesse*, 1989]. The result agrees very well with the earlier Voyager result of 2.2 × 10^{-3} as corrected to the Anders and Grevesse value of C/H [*Gautier and Owen*, 1989].

7.2. $^{13}C/^{12}C$ Isotopic Ratio

No NH_3 was expected to reach leak DL1 because of the sink provided by the interior surfaces of the inlet system. Thus we are not able to make any statement about the NH_3 abundance at pressures <8.9 bar from the DL1 measurements. The entire signal detected at 17 amu in DL1 (Figure 5b) can be accounted for by contributions from $^{13}CH_4$ and $^{12}CH_3D$. That being the case, the ratio of [17] to [16] in DL1 gives an isotopic ratio for ^{13}C to ^{12}C of 0.0108 ± 0.0005, which is precisely the solar system value [*Anders and Grevesse*, 1989]. The contribution of CH_3D to the ratio should only be about 1.5×10^{-4}.

7.3. Ammonia

In DL2 there was clearly a large contribution to [17] because of NH_3 outgassing from the walls of the ionization and detector chambers after the large releases of NH_3 from EC1 and EC2 (Figure 5b). Thus, only an upper limit to the NH_3 mixing ratio, 2.3×10^{-3}, can be derived from these observations, which is consistent with the observations by *Sromovsky et al.* [1996, this issue].

7.4. Water Vapor

The inlet walls at the vacuum side of DL1 adsorbed H_2O, as they did NH_3, and it is not clear whether they had become saturated by the time the direct leak was closed at 3.8 bars. If they had become saturated, the 18 amu signal observed can yield a water vapor mixing ratio in the DL1 region. To determine the H_2O mixing ratio, [18] must be corrected for a contribution from $^{36}Ar^{++}$. According to EU calibration data, this was 0.108 times [36]. The mixing ratio of water vapor at 2.7 bars would have been about 8×10^{-7} (^{16}O, 4.7×10^{-4} solar [*Anders and Grevesse*, 1989]) if the corrected ratio of [18] to [14] (Figure 5c) was attributable to atmospheric water vapor. However, if the inlet system was still removing water vapor from the gas sample before it could reach the ionization region, this would not even be an upper limit. That the apparent mixing ratio remained essentially constant throughout DL1 suggests that the walls, in fact, were not a problem, and the mixing ratio was indeed 8×10^{-7}.

Behavior similar to that at 17 amu was also observed at 18 amu in DL2, especially in DL2b after the second enrichment cell was sampled (Figure 5c). Thus, rigorously, for water vapor, as for ammonia, we can only set upper limits to the mixing ratios. These upper limits are about $(5.6 \pm 2.5) \times 10^{-5}$ between 8.7 and 11.7 bars in DL2a (^{16}O, 0.033 ± 0.015 solar) and about an order of magnitude greater at 18.7 bars in DL2b. The latter value is based on calibration carried out at a pressure <12 bar and will be provisional until the high-pressure exercise discussed in the calibration section has been accomplished. Even the mixing ratio deduced in DL2a at pressures <12 bar may have to be modified when calibration with a newly refurbished EU has been completed.

Data obtained by the Galileo orbiter 5 μm near infrared mapping spectrometer (NIMS) over "hot spots" like the one the probe entered agree with the low provisional mixing ratio observed by the GPMS at low pressures (<4 bars) as well as those observed (as upper limits) near 8 bars [*Carlson et al.*, 1996; *Carlson*, 1997; *Roos-Serote et al.*, this issue].

7.5. H_2S, PH_3, SiH_4, and Cl(?)

In DL2, constituents that are clearly atmospheric made contributions to the count rates at 31, 32, 33, and 34 amu (Figures 6d, 6e, and 6f). In DL1 H_2S was essentially undetectable with a mixing ratio of, at most, 7×10^{-7} ($^{32}S < 0.03$ times solar with solar photospheric $^{32}S/H = 1.54 \times 10^{-5}$ [*Anders and Grevesse*, 1989]). Analysis in DL2 is complicated by the possible presence of several plausible candidate species (Figure 6) whose ionization products would appear at these mass numbers: H_2S at 34, 33, and 32 amu; PH_3 at 31, 32, 33, and 34 amu; SiH_4 at 28, 29, 30, 31, and 32 amu; and hydrocarbons such as $^{13}C^{12}CH_6$ and $^{12}C_2H_5D$ at 31 amu. In fact, laboratory calibration studies with ethane revealed a contribution of 2×10^{-2} [30] at 31 amu. Removal of that contribution to the [31] count rate in the Jovian atmosphere leaves P from PH_3 and SiH_3 from silane as possible contributors at 31 amu. Preflight calibration data with the FU are available to provide the cracking patterns for PH_3 and SiH_4, so we can determine PH_3 contributions to the count rates at 32, 33, and 34 amu for any presumed PH_3 mixing ratio. We have both preflight FU and postflight EU calibration data for H_2S. Self-consistent sets of PH_3, SiH_4, and H_2S mixing ratios can be derived, depending on how much, within allowable limits, PH_3 and SiH_4 contributed to [31]. Table 3 shows details of such an exercise at 18.8 bars, where [31] has been reduced by 2×10^{-2} [30] (88 counts) and the H_2S mixing ratios that result from assuming PH_3 or, alternatively, SiH_4 contributed all, none, or a fraction of the resulting 111 counts at 31 amu. The permissible range in the H_2S mixing ratio was between 7.2 and 7.8×10^{-5} (^{32}S, 2.4–2.6 solar). The case of $PH_3 = 6 \times 10^{-7}$ (^{31}P, 0.8 solar) was selected because PH_3 with this mixing ratio has been detected for pressures greater than 1 bar by remote sensing [*Kunde et al.*, 1982; *Drossart et al.*, 1982; *Weisstein and Serabyn*, 1996]. Figure 6 shows the mixing ratio profiles for H_2S, PH_3, and SiH_4 that result from these assumptions. H_2S (Figure 6d) rose from 7×10^{-6} at 8.7 bars (0.23 solar) to a plateau between 7.2×10^{-5} and 7.8×10^{-5} (2.4–2.5 solar) from 15.7 to 18.7 bars. PH_3 had, at best, a very low mixing ratio, between 0 and $(2 \pm 1) \times 10^{-7}$ (^{31}P, 0.3 solar) at pressures less than 12 bars. At pressures greater than 15.7 bars its allowed mixing ratio was between 0 and 6.3×10^{-6} (^{31}P, 8.4 solar). Similarly, SiH_4 could have been, at most, 10^{-8} (^{28}Si, 1.5×10^{-4} solar) at pressures less than 12 bars and, at most, 1.1×10^{-7} (^{28}Si, 1.7×10^{-3} solar) at pressures greater than 15.7 bars. The absence of a detectable amount of SiH_4 would be consistent with thermochemical models [e.g., *Fegley and Lodders*, 1994]. We emphasize that the results reported here for the DL2b region are far less robust than those for DL2a because the environmentally induced alteration in the GPMS properties and the necessity of using a secondary reference, namely, [14]′ for [4]. Clearly, the analysis presented here does not demonstrate that PH_3 or SiH_4 were present at detectable levels. The mass spectrum obtained at about 18.8 bars, for example, can be reproduced with a model that contains only H_2S, Ar, and NMHCs as contributors to the spectrum between 31 and 40 amu. Whether the same mix can produce the observed spectra at other pressures remains to be seen.

In DL2 there were appreciable signals at 35 and 37 amu. Obvious candidate contributors are ^{35}Cl and ^{37}Cl. ^{33}S is 7.9×10^{-3} times as abundant as ^{32}S, so allowance for $H_2{}^{33}S$ must be made in the 35 amu count rates. The ratio of ([35] − 7.9×10^{-3} [34]) to [4] 69 [14]′ is plotted in Figure 6. The counting ratio of [37] multiplied by a factor of 4 to [4] and 81.3 [14]′ is also plotted. The same kind of gradient in mixing ratio that is characteristic of most volatiles, except CH_4 and the noble gases, is also in evidence here. The ratio of [37] to ([35] − 7.9×10^{-3} [34]) averaged 0.21 ± 0.07 between 8.6 and 12 bars

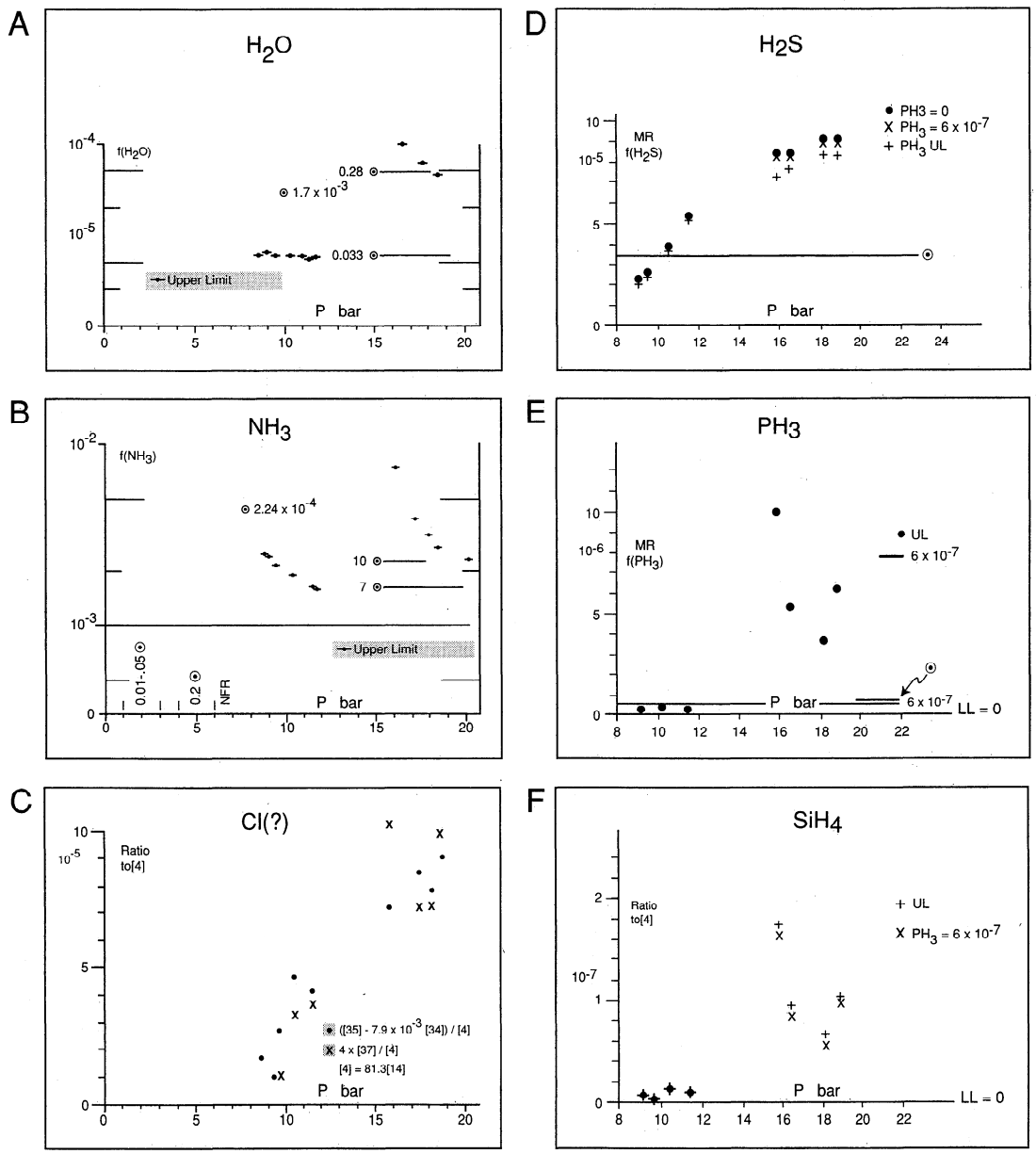

Figure 6. Mixing ratios of H_2O, NH_3, H_2S, PH_3 and the ratio of counts at 35 and 37 amu to those at 4 amu. The measured ratios at 17 and 18 amu are to be considered only as upper limits. The mixing ratios for H_2O for pressures greater than 15 bars are provisional until the sensitivity of the mass spectrometer has been determined at those pressures. Mixing ratio of H_2S corresponding to three assumptions regarding PH_3 and SiH_4 mixing ratios or count rate ratios. Below 12 bars there is presently an uncertainty of about 50% in the calibration of the instrument.

Table 3. Counts per Step at 31, 32, 33, and 34 amu for Three Consistent Sets of Mixing Ratios of PH_3, SiH_4, and H_2S

		PH_3			SiH_4			H_2S		
		$f \times 10^6$			$f \times 10^7$			$f \times 10^5$		
Mass	Total	0	0.6	6.2	1.08	0.98	0	7.8	7.7	7.2
31	107	0	10	107	107	97	0			
32	3,124	0	66	710	6	5	0	3,118	3,053	2,144
33	3,048	0	18	190	0	0	0	3,048	3,090	2,858
34	10,700	0	74	793	0	0	0	10,700	10,626	9,907

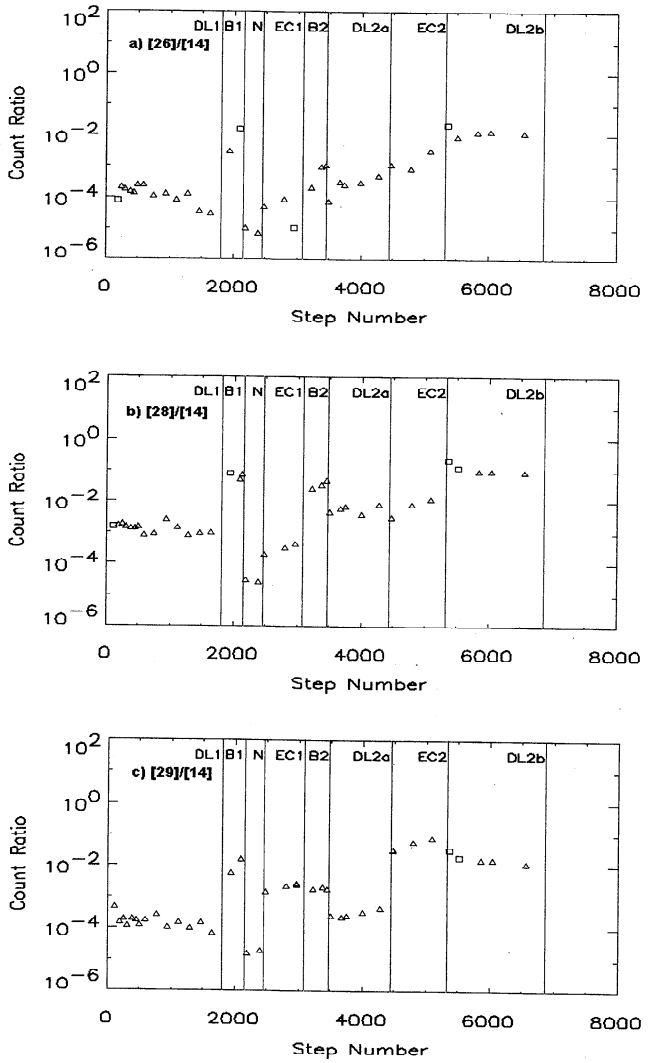

Figure 7. Count ratios to 14 amu at (a) 26, (b) 28 (c) 29, (d) 30, (e) 32, (f) 34, (g) 43, and (h) 44 amu.

and 0.33 ± 0.15 between 15.7 and 21 bars. The solar $^{37}Cl/^{35}Cl$ ratio is 0.32.

8. Nonmethane Hydrocarbons

There were species that produced fairly sizeable counting rates between 24 and 30 amu, which could have been C_2 hydrocarbons, and between 39 and 44 amu, which is the domain of C_3 hydrocarbons (Figures 7c, 7d, 7e, and 7h). Low, but detectable rates were also found above 50 amu, which might be attributable to C_4 hydrocarbons (Figure 3). Of course, other species as well are possible, even if implausible, at some of these mass numbers. For example, contributions at 74, 76, and 78 amu could be from hydrocarbons such as C_6H_6 and from GeH_4. The profiles with depth seem to be of three types. The first type of profile is the one characteristic of species like Ne and Ar, where the abundance varies little with pressure. The second is typically that of the volatile species at 31, 33, 34, 35, and 37 amu whose abundances decreased monotonically with decreasing pressure. The third is represented by the species at 26, 27, 28, 29, 32, and 39 amu, at which masses hydrocarbons are expected to dominate. Complete analysis identifying the species in this third class and determining their abundances has not yet been finished. However, their altitude dependence is certainly unexpected if they are hydrocarbons in Jupiter's atmosphere. In that case, they are expected to be produced photochemically from CH_4 at high altitude, to diffuse downward and recombine to re-form CH_4 near the 300 bar level [*Lewis and Fegley*, 1984]. And, indeed, at pressures below 3 bars the counting rates for species with mass numbers such as 26, 27, 29, 39, and 43 amu did increase with decreasing pressure. However, they also increased again to very high values with increasing pressure until they reached an apparent plateau at pressures greater than 15.5 bars (Figures 7a–e and 7h) in DL2b. The possibility that the hydrocarbons observed, especially those at high altitude, were internally generated needs to be explored.

The value [28] is much too large to be C_2H_4 alone. To what extent it arises from N_2 or CO, terrestrial or Jovian, remains to be seen.

9. Other Species: 23, 40, and 44 amu

The mass peak at 23 amu was definitely surface ionized sodium of instrumental origin. The enrichment chamber tests at 15 and 25 eV indicate that the responsible species has a low ionization potential. It is very unlikely that it could have been

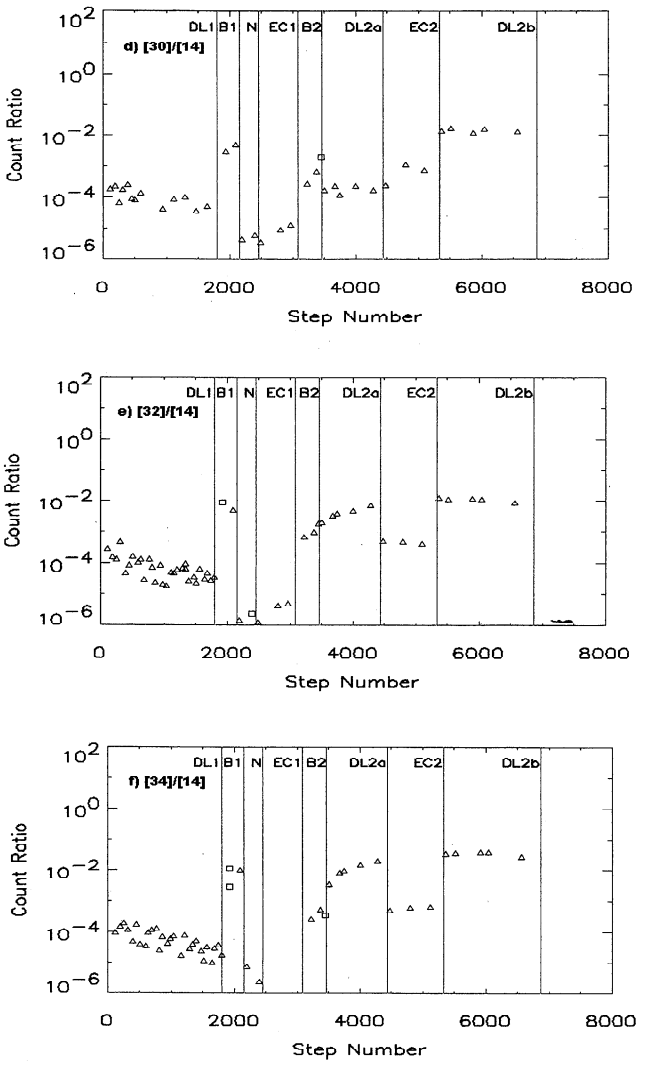

Figure 7. (continued)

Jovian, given the extreme difficulty sodium would have had in making its way through the inlet system. Sodium is a familiar contaminant in mass spectrometers.

Most of the counts at 44 amu must be attributed to something other than propane because the ratio of [44] to [43] was 1 to 2 orders of magnitude larger than it should have been if these were ionization products of C_3H_8. The only other reasonable candidate is CO_2. The [45]/[44] ratio is broadly consistent with that identification, where [45] would have come mainly from $^{13}CO_2$. The CO_2 was probably of terrestrial origin, released from getter pumps and enrichment cells in a pressure-dependent fashion. According to recent observations at 14.98 μm from the Infrared Space Observatory [*Feuchtgruber et al.*, 1997], the stratospheres of Saturn and Neptune contain only 0.3 and 0.5 ppb of CO_2, respectively. Saturation effects prevented measurements at Jupiter, but the mechanism for production of CO_2, the same for all three planets, should produce less than 0.1 ppb of CO_2 on Jupiter. Like sodium, CO_2 is often found as a contaminant in mass spectrometers.

Similarly, the signal at 40 amu was terrestrial argon, the residue of argon introduced during welding, and cannot have been mainly C_3H_4.

10. Discussion and Conclusions

Table 1 summarizes our results and compares them with other measurements.

10.1. $^4He/H_2$

H_2 and He in the protosolar cloud should not have been incorporated in ices or other solids that formed the core of Jupiter or that arrived later, after the planet began to accrete gas from the nebula. Thus the atmospheric $^4He/H_2$ and Ne/H_2 ratio should originally have been protosolar. However, after the planet divided into an outer convective envelope and a metallic interior, a phase transition should have occurred at the 3 M bar level, in which helium condensed out of the binary He-H_2 system. Since the helium drops are heavier than the hydrogen-rich phase around them, they should have rained out to the level at which the temperature and pressure became high enough for them to dissolve again. The circulation system of helium rain and convection should have depleted the atmosphere of helium. That the atmospheric $^4He/H_2$ ratio is 0.157, as measured by the probe instruments, instead of the higher protosolar value of 0.21–0.29 is evidence that this process has occurred on Jupiter as it must have to an even more pronounced degree, on Saturn [*Stevenson and Salpeter*, 1977]. This result is in excellent agreement with that of the HAD in the probe payload [*von Zahn et al.*, this issue]. The underabundance of neon may well be caused by incorporation of neon atoms preferentially in the helium phase, as predicted by *Roulston and Stevenson* [1995].

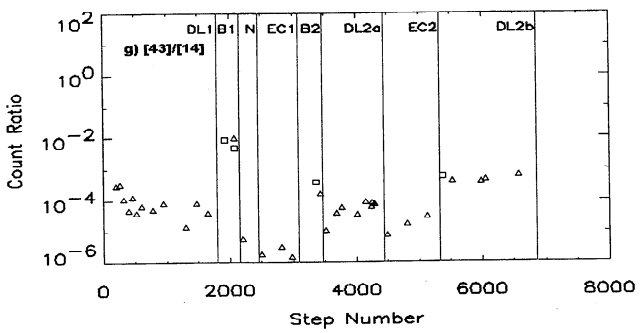

Figure 7. (continued)

Table 4. Ratio (D + ^{3}He)/H at Jupiter and in the Local Interstellar Medium

	(D + ^{3}He)/H	Time
Jupiter	$(4.3 \pm 1.6) \times 10^{-5}$	−4.6 Gyr
LISM	$(4.1 \pm 1.0) \times 10^{-5}$	now

10.2 D/H and $^3He/^4He$

The value of the deuterium to hydrogen ratio in Jupiter's atmosphere is very important for an understanding of nucleosynthesis and the evolution of light elements in the galaxy resulting from nuclear processing in stellar interiors. Because Jupiter's hydrogen and helium should have been acquired predominantly from the solar nebula either during or shortly after the time the Sun was formed, the D/H and $^3He/^4He$ ratios should be those prevailing in the part of the universe where the solar system originated about 4.6 Gyr ago. They can be compared with similar ratios measured in the nearby interstellar medium today. In hydrogen gas in the local interstellar medium (LISM), D/H = $1.6 \pm 0.2 \times 10^{-5}$ [*Linsky*, 1996], indicating that this ratio has decreased modestly from the Jovian value of D/H = $2.6 \pm 0.7 \times 10^{-5}$ in the last 4.6 Gyr. This decrease is expected from the steady conversion of D to ^{3}He in stellar interiors. In principle, therefore, the sum (D + ^{3}He)/H should be constant with time in a given region of the interstellar medium. *Gloeckler and Geiss* [1998] reported $^3He/H = (2.48 + 0.85, -0.79) \times 10^{-5}$ in the LISM from an analysis of He ions entering the solar system as detected by the ion composition spectrometer on the Ulysses spacecraft. Table 4 summarizes these results.

Within the large uncertainties, it indeed appears that there has been little, if any, change. Furthermore, the modest change in D/H in 4.6 Gyr is consistent with values of D/H of several times 10^{-5} just after the Big Bang, as measured in highly red shifted Lyman α clouds illuminated by quasars. This would imply that a large population of baryons was produced in the primordial fireball, consuming much of the deuterium generated then. The Jovian value of $^3He/^4He = (1.66 \pm 0.05) \times 10^{-4}$ agrees closely with the meteoritic value of $(1.5 \pm 0.3) \times 10^{-4}$. This indicates that possible fractionation processes during the trapping of helium in the meteorites or the raining out of helium in Jupiter's interior have had a small effect.

10.3. H_2O, H_2S, and NH_3: Implications for Local Meteorology

One striking feature of H_2S and H_2O measured by GPMS, and of NH_3 measured by other instruments, is that these species were all greatly depleted in the Galileo probe entry region to depths well below their expected condensation levels. Their mixing ratios, however, are found to increase gradually with depth, perhaps eventually recovering to their normal deep atmospheric abundances. All of these gases are expected to condense either directly or via thermochemistry in the atmosphere of Jupiter. Prior to Galileo, however, only the existence of the topmost cloud of ammonia ice had been confirmed. The negative Galileo results on the other potential clouds were initially surprising but are understandable when one considers the behavior of the condensable volatiles along the probe trajectory.

The GPMS upper limit on the H_2S mixing ratio of 6×10^{-7} at pressures of 4 bars or less in DL1 is surprising, since the condensation level should lie at 2.2 bars for solar S/H and 2.7 bars for 3 times solar S/H [*Atreya and Romani*, 1985; *Weidenschilling and Lewis*, 1973]. Previously, *Larson et al.* [1984] noted a global depletion of H_2S at pressures less than 0.8 bar from their Earth-based 2.7 μm observations, but this was expected because H_2S should be removed after reaction with NH_3 followed by condensation of the products deeper in the atmosphere. Note that H_2S itself cannot condense in the Jovian atmosphere; its reaction with NH_3, however, produces ammonium hydrosulfide (NH_4SH) or, as proposed by *Owen and Mason* [1969], ammonium sulfide $(NH_4)_2S$, which do solidify at the prevalent temperatures. Although the GPMS did not detect H_2S in the 4–8 bar region because it was not sampling the atmosphere there, the measurements carried out from 8 to 20 bars revealed a gradual rise (Figure 6d) in the H_2S mixing ratio from 0.23 times solar at 8.7 bars to about 2.5 times solar at approximately 16 bars. The indication is that H_2S has leveled off at this last value for depths beyond 16 bars; this conclusion should, however, be interpreted with caution until pressure-dependent calibrations with the refurbished EU have been completed. Nevertheless, the trend with depth, i.e., depletion of H_2S to pressures well below its expected condensation level and the gradual buildup in its mixing ratio with increasing depth, eventually recovering to its normal deep atmospheric value, is expected to hold. Note that the degree of enrichment of sulfur is essentially identical to that of carbon in Jupiter's atmosphere: both have about 3 times their solar values.

As for the absolute mixing ratio of water vapor in the deep atmosphere, the GPMS analysis is still tentative. There is a strong suggestion (Figure 5) that the water vapor mixing ratio, like that of H_2S, increased with depth by nearly a factor of 10 between 10 and 20 bars. Like H_2S, water vapor seems to be greatly depleted to pressures well below its expected condensation levels of 5.4–6.5 bars (for solar and 2 solar O/H [*Atreya and Romani*, 1985; *Weidenschilling and Lewis*, 1973]). Unlike H_2S, however, H_2O does not appear to achieve a constant mixing ratio at the highest pressures reached by the GPMS. At pressures of 4 bars or less, the provisional mixing ratio from the GPMS analysis of 8×10^{-7} corresponds to 1% saturation at 4 bars.

The best results on the behavior of ammonia with depth are currently available from instruments other than GPMS. The net flux radiometer (NFR) data can be most reasonably interpreted with ^{14}N from NH_3 between 1 to 2 times solar at 3–6 bars [*Sromovsky et al.*, 1996, this issue]. However, the NH_3 mixing ratio must have been lower at 1 bar than at 3 bars by a factor of 20 to 5–10% solar (i.e., a mixing ratio of $1–2 \times 10^{-5}$), whereas clouds are not expected to form until the pressure decreases to approximately 0.7 bar (for solar N/H [*Atreya and Romani*, 1985]). The NFR data also require that NH_3 must have dropped by another factor of 4, i.e., to 1–2% solar (a mixing ratio of $2–4 \times 10^{-6}$), between 1 and 0.5 bar. The depletion in ammonia at low pressures has also been confirmed by the NIMS observations [*Carlson et al.*, 1996; *Roos-Serote et al.*, this issue], while an increase of the mixing ratio with pressure to 3.3 times solar at about 9 bars was obtained from the analysis of the strength of the probe's signal at the orbiter [*Folkner et al.*, this issue]. This is in conflict with the numerous microwave and radio measurements with the very large array (VLA), which yield a globally averaged value of N/H = 1.3 times solar in Jupiter's atmosphere [e.g., *de Pater and Massie*, 1985]. It suggests that the depth at which NH_3 may have recovered to its normal deep atmospheric value was at a pressure higher than is implied by the NFR data.

This behavior of the condensable volatiles with depth along the probe's trajectory can be the result of local meteorology. The probe entry region is believed to have been the region of a downdraft [*Carlson et al.*, 1993; *Niemann et al.*, 1996; *Atreya et al.*, 1996, 1997; *Owen et al.*, 1996, 1997; *Showman and Ingersoll*, 1996, 1998; D. M. Hunten et al., Dissipation of Jovian water clouds due to subsidence, submitted to *Icarus*, 1998; hereinafter referred to as submitted paper]. The condensable volatiles were largely removed from an updraft cell, first by condensation and then by sedimentation preceded by particle growth due to coagulation and coalescence. The mixing ratios are limited even further if the air mass rose above the lifting condensation levels, so much so that at Jupiter's 110 K tropopause, virtually all of the condensable volatiles had been removed from the atmosphere. If this air mass were allowed to descend as a downdraft into the probe entry region, it would have mixed with the probe-region atmosphere. This would then have resulted in the gradual recovery with depth in the condensable volatile mixing ratios, precisely what has been observed. To have driven this downdraft and kept it dry to such great depths, *Showman and Ingersoll* [1996, 1998] proposed a thermodynamic heat engine in reverse. Considering Jupiter's large internal heat, it seems surprising that the condensable volatiles did not all recover at the same depth, say, below the purported water cloud levels. This may perhaps have been due to entrainment of adjacent, well-mixed Jovian air into the probe entry region [*Atreya et al.*, 1997]. Finally, the nearly cloud-free trajectory of the probe [*Ragent et al.*, 1996, this issue] can be easily understood in view of the measured abundances of the condensables. No evidence of any massive cumulus-type clouds was found in the nephelometer data. The concentrations of the very tenuous clouds at 0.5 and 1.34 bars, and an even more tenuous layer at 1.65 bars [*Ragent et al.*, 1996, this issue] are entirely consistent with an NH_3-ice cloud at 0.5 bar (or lower pressure), an NH_4SH-solid cloud at 1.34 bars, and a very thin H_2O ice cloud at 1.65 bars [*Atreya et al.*, 1997] when one considers the depleted levels of the condensables measured on the probe. In addition, only a modest downdraft velocity of a few m/s is sufficient to dissipate a water ice cloud even for O abundances as great as 20% of solar (D. M. Hunten et al., submitted paper, 1998).

10.4. NMHC Peaks

All the peaks potentially belonging to C_2 and C_3 hydrocarbons share the general behavior of showing high count rates at 1 bar, falling to a very low mixing ratio at pressures of about 3 bars, and rising to a much higher value by 15 bars. There are no direct leak data for the ambient atmosphere between 11 and almost 15 bars because of the addition of the EC2 sample to the DL2 sample. There have been prior suggestions that higher order hydrocarbons which are produced photochemically in the stratosphere may condense near the temperature minimum of the tropopause [*Atreya*, 1986]. They would be expected to reevaporate as they are mixed downward to deeper and warmer levels. However, the temperatures at which such reappearance is observed are much warmer than expected for such simple evaporation (339 K at 10 bars and 380 K at 15 bars). A thermochemical source deep in the atmosphere is not feasible. Temperatures never attain the level required to produce hydrocarbon products from CH_4 in the gaseous interior of the planet. A possible explanation is that the molecules are tightly adsorbed or absorbed to the hydrocarbon particles that are also produced in the stratosphere. Like the simpler molecules, their fate is to mix downward to a region that is warm enough to decompose them and add H atoms to convert them back to CH_4, around 1000 K and 300 bars according to *Lewis and Fegley* [1984]. However, it cannot be excluded that the apparent increase in ethane and propane abundance with pressure is an instrumental artifact involving their generation by an internal mechanism. Until this possibility has been thoroughly investigated, these results should be treated with caution.

10.5. Origin of the Atmosphere

The currently favored model of the formation of the giant planets is the nucleation and collapse model [*Mizuno*, 1980; *Pollack and Bodenheimer*, 1989]. According to this model, the core consisting of rock and ice formed first. When the mass of the core grew to be sufficiently large, it began to attract the solar nebula gas, eventually leading to the collapse of the circumplanetary nebula. Bombardment by planetesimals would continue even beyond this phase. The atmosphere therefore resulted from three components: the volatiles released from the core during accretionary heating, those released by infalling planetesimals dissolving in the gaseous envelope [*Pollack and Bodenheimer*, 1989], and those contributed directly by the solar nebula. This scenario implies that those elements whose volatile compounds were initially trapped in the planetesimals that produced the core and dissolved in the envelope should have enhanced abundances in the atmosphere. The solar nebula component can be well understood by measuring the elemental abundances in the Sun. For the planetesimal contribution, observations of the interstellar medium (ISM), the volatile-rich meteorites and the comets combined with laboratory data are helpful.

In the interstellar medium the reservoir of carbon is mostly in the form of grains and refractory organics, not volatiles such as CO and CH_4. On the other hand, nitrogen is mostly in the volatile form, N_2 [e.g., *Irvine and Knacke*, 1989; *van Dishoeck et al.*, 1993]. Most of the comets in the Oort cloud originally formed at 55 ± 15 K in the vicinity of Uranus and Neptune. At these temperatures, ice does not trap N_2, CO, and CH_4 well but easily traps refractory organics and NH_3 as well as compounds of the other heavy elements [*Bar-Nun et al.*, 1985, 1988]. Unless the temperature is below 25 K, it does not trap H_2, He, or Ne. These gases are not captured easily in rocks either, so in Jupiter's atmosphere, we expect H, He, and Ne to be contributed only by solar nebula gas and therefore to exhibit solar relative abundances. The observed depletion of helium and neon in the atmosphere [*Niemann et al.*, 1996] is most likely due to the loss of helium to condensation in the planet's interior and the fractionation of neon into helium droplets [*Stevenson and Salpeter*, 1977; *Roulston and Stevenson*, 1995]. Contribution of nitrogen to the atmosphere by the core and by infalling planetesimals should also be small. Thus little enhancement in the nitrogen elemental ratio is expected. On the other hand, considerable enrichment in the abundances of carbon, sulfur, and oxygen should occur.

The probe mass spectrometer measured C/H = 2.9 solar, in accord with ground-based and Voyager results. It also measured sulfur, in the form of H_2S, for the first time and found that the S/H at the deepest level probed (20 bars) is 2.5 solar. The nearly equal enrichment of carbon and sulfur is consistent with the predictions of a model in which icy planetesimals make the major contribution of heavy elements [*Owen and Bar-Nun*, 1995]. Even in carbonaceous chondrites, the most carbon rich of the meteorites, C/S = 0.1 solar. Unless there are "rocky" bodies unsampled by our collection of meteorites, it appears that only icy planetesimals have the correct composition to enrich these elements almost equally [*Owen et al.*, 1997]. The icy planetesimal model also predicts that oxygen (as H_2O) should be similarly enhanced, perhaps even slightly more than carbon [*Owen and Bar-Nun*, 1995]. Unfortunately, the probe mass spectrometer data for H_2O cannot yet reveal the H_2O mixing ratio at the deepest atmospheric level probed, and it does not appear that H_2O has even recovered to its "normal" non-hot-spot value at this level. However, the 5 μm observations by the orbiter NIMS show a stark contrast between the hot spot and the regions outside, with preliminary indications that the H_2O mixing ratio begins to recover in the regions outside hot spots [*Carlson*, 1997; M. Roos-Serote et al., Constraints on the tropospheric cloud structure of Jupiter from spectroscopy in the 5 micron region: A comparison between Voyager/IRIS, Galileo/NIMS, and ISO/SWS spectra, submitted to *Icarus*, 1998; hereafter referred to as submitted paper]. Previously, *Carlson et al.* [1993] obtained a best fit to the Voyager infrared imaging spectrometer (IRIS) H_2O data with ^{16}O twice solar in abundance. (This result could be controversial, according to a recent reanalysis of the IRIS data by M. Roos-Serote et al. (submitted paper, 1998).)

This apparent concordance of model predictions and observations runs into trouble with nitrogen [*de Pater and Massie*, 1985]. If the analysis of *Folkner et al.* [this issue] is correct, it suggests that nitrogen is at least as enriched as carbon and sulfur in Jupiter's atmosphere. This would require that the solid planetesimals bring in nitrogen, carbon, and sulfur in the same proportions we find them in the Sun, and we know of no planetesimals that have this solar composition. The comets whose composition we have measured are deficient in nitrogen [*Krankowski*, 1993], which we can understand in terms of the inability of condensing ice to trap N_2 efficiently unless the ambient temperature is $\leq$35 K [*Owen and Bar-Nun*, 1995]. Thus a value of N on Jupiter of approximately 3 times solar would require building up the core and/or dominating the infalling ices with comets from the Kuiper Belt, or with solid material coming directly from the interstellar cloud that formed the solar system, without sublimation and recondensation as described by *Lunine et al.* [1991].

If this is what happened, argon, krypton, and xenon should

be similarly enriched. Otherwise, we would expect them to be present in solar proportions, dominated by the contribution from the solar nebula. We must await mixing ratios for both Kr and Xe to test this point. However, at this stage, we feel we can already rule out clathrate hydrate structures in the cometary ice as volatile carriers based on the predictions of *Lunine and Stevenson* [1985]. Extrapolating from their published calculations for the enrichment of Xe and Kr as a function of the enrichment of carbon, we find for $C/H_2 = 3$ solar, $Xe/Ar > 9$ solar for the least enhanced cases (structure I clathrate, CH_4 dominant; structure II clathrate, CO dominant). Instead, the GPMS results give $Xe/Ar \leq 5$ in Jupiter's atmosphere.

Acknowledgments. We thank J. Cooley for his efforts as instrument manager, R. Lott and T. Tyler for the mechanical design contributions, A. Doan for help in the enrichment cell design, R. Abell, H. Powers, and H. Mende for the precision assembly welding and machining, and R. Arvey and H. Benton for the electronics assembly and testing at GSFC. The contributions to the electronics system design of B. Block, J. Caldwell, J. Eder, J. Maurer, and W. Pinkus at the University of Michigan are gratefully acknowledged. The hybrid electronic circuits were fabricated at the General Electric Astro Space Division at Valley Forge, Pennsylvania, and the microvalves for the gas sampling system were designed and fabricated by Energy Research and Generation, Inc., in Oakland, California. The chemical getter material was provided by SAES Getter of Milan, Italy, and the capillary leaks and secondary electron multipliers were manufactured by Galileo Electro Optics in Strubridge, Massachusetts. M. Wong of the University of Michigan significantly contributed to data analysis and instrument calibration. We also thank the Galileo probe project personnel at NASA Ames Research Center, and we particularly acknowledge the contributions of A. Wilhelmi, C. Sobeck, and P. Melia for their efforts during the development, spacecraft integration, and testing phases. A special thank you is owed Jan Beltran at the University of Michigan for her efforts during the preparation of this manuscript. The GPMS experimenters dedicate this paper to Nelson Spencer, who made such a great contribution to spacecraft mass spectroscopy and was an inspirational leader during the early stages of this project.

References

Anders, E., and N. Grevesse, Abundances of the elements: Meteoritic and solar, *Geochim. Cosmochim. Acta*, *53*, 197–214, 1989.

Atreya, S. K., *Photochemistry, Atmospheres and Ionospheres of the Outer Planets and Their Satellites*, chap. 5, Springer-Verlag, New York, 1986.

Atreya, S. K., and P. N. Romani, Photochemistry and clouds of Jupiter, Saturn, and Uranus, in *Recent Advances in Planetary Meteorology*, edited by G. E. Hunt, pp. 17–68, Cambridge Univ. Press, New York, 1985.

Atreya, S. K., T. C. Owen, M. Wong, H. B. Niemann, and P. Mahaffy, Condensible volatiles, clouds, and implications for meteorology in the Galileo probe entry region: Jupiter is not dry!, *Bull. Am. Astron. Soc.*, *28*(3), 1133, 1996.

Atreya, S. K., M. Wong, T. C. Owen, H. B. Niemann, and P. Mahaffy, Chemistry and clouds of the atmosphere of Jupiter: A Galileo perspective, in *Three Galileos: The Man, The Spacecraft, The Telescope*, edited by J. Rahe et al., pp. 249–260, Kluwer Acad., Norwell, Mass., 1997.

Bar-Nun, A., G. Herman, D. Laufer, and M. L. Rappaport, Trapping and release of gases by water, ice and implications for icy bodies, *Icarus*, *63*, 317–332, 1985.

Bar-Nun, A., I. Kleinfeld, and E. Kochavi, Trapping of gas mixtures by amorphous water ice, *Phys. Rev. B*, *38*, 7749–7754, 1988.

Black, D. C., On the origins of trapped helium, neon, and argon isotopic variations in meteorites, I, *Geochim. Cosmochim. Acta*, *36*, 347, 1972.

Carlson, B. E., A. A. Lacis, and W. B. Rossow, Tropospheric gas composition and cloud structure of the Jovian north equatorial belt, *J. Geophys. Res.*, *98*, 5251–5290, 1993.

Carlson, R., Near-IR spectroscopy of the atmosphere of Jupiter, paper presented at the XXIII General Assembly, Int. Astron. Union, Kyoto, Japan, August 21, 1997.

Carlson, R., et al., Near infrared spectroscopy and spectral mapping of Jupiter and the Galilean satellites: Results from Galileo's initial orbit, *Science*, *274*, 385–388, 1996.

dePater, I., and S. T. Massie, Models of the millimeter-centimeter spectra of the giant planets, *Icarus*, *62*, 143–171, 1985.

Drossart, P., T. Encrenaz, V. Kunde, R. Hanel, and M. Combes, An estimate of the PH_3, CH_3D, and GeH_4 abundances on Jupiter from the Voyoger IRIS data at 4.5 microns, *Icarus*, *49*, 416–426, 1982.

Eberhardt, P., A neon-E-rich phase in the Orgueil carbonaceous chrondrite, *Earth Planet. Sci. Lett.*, *24*, 182, 1974.

Encrenaz, T., E. Zellouch, B. Bezard, P. Drossart, M. Roos-Serote, and D. A. Naylor, First results of ISO-SWS observations of Jupiter, *Astron. Astrophys.*, *315*, L397–402, 1996.

Fegley, B., and K. Lodders, Chemical models of the deep atmospheres of Jupiter and Saturn, *Icarus*, *110*, 117–154, 1994.

Feuchtgruber, H., E. Lellouch, T. de Grauw, B. Bezard, T. Encrenaz, and M. Griffin, External source of oxygen in the atmospheres of the giant planets, *Nature*, *389*, 159–162, 1997.

Folkner, W. M., R. Woo, and S. Nandi, Ammonia abundance in Jupiter's atmosphere derived from the attenuation of the Galileo probe's radio signal, *J. Geophys. Res.*, this issue.

Gautier, D., and T. Owen, The composition of outer planet atmospheres, in *Origin and Evolution of Planetary and Satellite Atmospheres*, edited by S. K. Atreya et al., pp. 487–512, Univ. of Ariz. Press, Tucson, 1989.

Geiss, J., Primordial abundance of hydrogen and helium isotopes, in Origin and Evolution of the Elements, edited by N. Prantzos, L. Vangioni-Flam, and M. Casse, pp. 89–106, Cambridge Univ. Press, New York, 1993.

Geiss, J., and G. Gloeckler, Abundances of deuterium and helium 3 in the protosolar cloud from solar wind measurement, *Space Sci. Rev.*, in press, 1998.

Gloeckler, G., and J. Geiss, Measurement of the abundance of helium-3 in the local interstellar cloud and the Sun, *Space Sci. Rev.*, in press, 1998.

Irvine, W. M., and R. F. Knacke, The chemistry of interstellar gas and grains, in *Origin and Evolution of Planetary and Satellite Atmospheres*, edited by S. K. Atreya, J. B. Pollack, and M. S. Matthews, pp. 3–34, Univ. of Ariz. Press, Tucson, 1989.

Krankowski, D., The composition of comets, in *Comets in the Post-Halley Era*, vol. 2, edited by R. L. Newburn Jr., M. Neugebauer, and J. Rahe, pp. 855–877, Kluwer Acad., Norwell, Mass., 1993.

Kunde, V. G., R. A. Hanel, W. Maguire, D. Gautier, J. P. Baluteau, A. Maarten, A. Chedia, N. Husson, and N. Scott, The tropospheric gas composition of Jupiter's north equatorial belt (NH_3, PH_3, CH_3D, GeH_4, H_2O) and the Jovian D/H isotopic ratio, *Astrophys. J.*, *263*, 443–467, 1982.

Larson, H. P., D. S. Davis, R. Hoffman, and G. Bjoraker, The Jovian atmospheric window at 2.7 μm: A search for H_2S, *Icarus*, *60*, 621–639, 1984.

Lewis, J. S., and M. Fegley Jr., Vertical distribution of disequilibrium species in Jupiter's troposphere, *Space Sci. Rev.*, *39*, 163–192, 1984.

Linsky, J. L., GHRS observations of the LISM, *Space Sci. Rev.*, *78*, 157–164, 1996.

Lunine, J., and D. J. Stevenson, Thermodynamics of clathrate hydrate at low and high pressures with application to the outer solar system, *Astrophys. J. Suppl.*, *58*, 493–531, 1985.

Lunine, J., S. Engel, B. Rizk, and M. Horanyi, Sublimation and reformation of icy grains in the primitive solar neubla, *Icarus*, *94*, 333–344, 1991.

Mahaffy, P. R., T. M. Donahue, S. K. Atreya, T. C. Owen, and H. B. Niemann, Galileo probe measurements of D/H and $^3He/^4He$ in Jupiter's atmosphere, *Space Sci. Rev.*, in press, 1998.

Mizuno, H., Formation of the giant planets, *Progr. Theor. Phys.*, *64*, 544–557, 1980.

Niemann, H. B., D. N. Harpold, S. K. Atreya, G. R. Carignan, D. M. Hunten, and T. C. Owen, Galileo probe mass spectrometer experiment, *Space Sci. Rev.*, *60*, 111–142, 1992.

Niemann, H. B., et al., The Galileo probe mass spectrometer: Composition of Jupiter's atmosphere, *Science*, *272*, 846–849, 1996.

Owen, T., and A. Bar-Nun, Comets, impacts, and atmospheres, *Icarus*, *116*, 215–226, 1995.

Owen, T. C., and H. P. Mason, New studies of Jupiter's atmosphere, *J. Atmos. Sci.*, *26*, 870–873, 1969.

Owen, T. C., S. K. Atreya, H. B. Niemann, and P. Mahaffy, The composition of Jupiter's atmosphere: Implications for origin, *Eos Trans. AGU*, *77*(46), Fall Meet. Suppl., F438, 1996.

Owen, T. C., S. K. Atreya, P. Mahaffy, H. B. Niemann, and M. H. Wong, On the origin of Jupiter's atmosphere and the volatiles on the Medicean stars, in *Three Galileos: The Man, The Spacecraft, The Telescope*, edited by J. Rahe, et al., pp. 289–298, Kluwer Acad., Norwell, Mass., 1997.

Pepin, R. O., On the origin and early evolution of terrestrial planet atmospheres and meteoric volatiles, *Icarus*, *92*, 2–79, 1991.

Pollack, J. B., and P. Bodenheimer, Theories of the origin and evolution of the giant planets, in *Origin and Evolution of Planetary and Satellite Atmospheres*, edited by S. K. Atreya, J. B. Pollack, and M. S. Matthews, pp. 564–604, Univ. of Ariz. Press, Tucson, 1989.

Ragent, B., D. S. Colburn, P. Avrin, and K. A. Rages, Results of the Galileo probe nephelometer experiment, *Science*, *272*, 854–855, 1996.

Ragent, B., D. S. Colburn, K. A. Rages, T. C. D. Knight, P. Arvin, G. S. Orton, P. A. Yanamandra-Fisher, and G. W. Grams, The clouds of Jupiter: Results of the Galileo Jupiter Mission Probe Nephelometer Experiment, *J. Geophys. Res.*, this issue.

Roos-Serote, M., et al., Analysis of Jupiter NEB hot spots in the 4–5 μm range from Galileo NIMS observations: Measurements of cloud opacity, water, and ammonia, *J. Geophys. Res.*, this issue.

Roulston, M. S., and D. J. Stevenson, Prediction of neon depletion in Jupiter's atmosphere (abstract), *Eos Trans. AGU*, *76*(46), Fall Meet. Suppl., F343, 1995.

Showman, A. P., and A. P. Ingersoll, Deep dry downdraft as an explanation for low Jovian water observations, *Bull. Am. Astron. Soc.*, *28*(3), 1141, 1996.

Showman, A. P., and A. P. Ingersoll, Interpretation of Galileo probe data and implications for Jupiter's dry downdrafts, *Icarus*, in press, 1998.

Sromovsky, L. A., F. A. Best, A. D. Collard, P. M. Fry, H. E. Revercomb, R. S. Freedman, G. S. Orton, J. L. Hayden, M. G. Tomasko, and M. T. Lemmon, Solar and thermal radiation in Jupiter's atmosphere: Initial results of the Galileo probe net flux radiometer, *Science*, *272*, 851–853, 1996.

Sromovsky, L. A., A. D. Collard, P. M. Fry, G. S. Orton, M. T. Lemmon, M. G. Tomasko, and R. S. Freedman, Galileo probe measurements of thermal and solar radiation fluxes in the Jovian atmosphere, *J. Geophys. Res.*, this issue.

Stevenson, D., and E. E. Salpeter, The dynamics and helium distribution in hydrogen-helium fluid planets, *Astrophys. J. Suppl.*, *35*, 221–239, 1977.

van Dishoeck, E. F., G. A. Blake, B. T. Draine, and J. I. Lunine, The chemical evolution of protostellar and protoplanetary material, in *Protostars and Planets III*, edited by E. H. Levy and J. I. Lunine, pp. 163–241, Univ. of Ariz. Press, Tucson, 1993.

von Zahn, V., and D. M. Hunten, The helium fraction in Jupiter's atmosphere, *Science*, *272*, 849–852, 1996.

von Zahn, V., D. M. Hunten, and G. Lehmacher, Helium in Jupiter's atmosphere: Results from the Galileo Probe Helium Interferometer Experiment, *J. Geophys. Res.*, this issue.

Weidenschilling, S. J., and J. S. Lewis, Atmospheric and cloud structure of the Jovian planets, *Icarus*, *20*, 465–476, 1973.

Weisstein, E. W., and E. Serabyn, Submillimeter line search in Jupiter and Saturn, *Icarus*, *123*, 23–36, 1996.

S. K. Atreya, G. R. Carignan, and T. M. Donahue, Department of Atmospheric, Oceanic and Space Sciences, University of Michigan, 2455 Hayward Street, Ann Arbor, MI 48109. (e-mail: tmdonahue@umich.edu)

J. A. Haberman, D. N. Harpold, R. E. Hartle, W. T. Kasprzak, P. R. Mahaffy, H. B. Niemann, and S. H. Way, Goddard Space Flight Center, Greenbelt, MD 20771.

D. M. Hunten, Lunar and Planetary Laboratory, University of Arizona, Tucson, AZ 85721.

T. C. Owen, Institute for Astronomy, University of Hawaii, 2680 Woodlawn Drive, Honolulu, HI 96822.

(Received October 1, 1997; revised March 13, 1998;
accepted March 23, 1998.)